Properties of Palmitoyl Phosphatidylcholine, Sphingomyelin, and Dihydrosphingomyelin Bilayer Membranes as Reported by Different Fluorescent Reporter Molecules

Thomas Nyholm, Matts Nylund, Annu Söderholm, and J. Peter Slotte
Department of Biochemistry and Pharmacy, Åbo Akademi University, FIN 20521 Turku, Finland

ABSTRACT   The properties of vesicle membranes prepared from 16:0-SM, 16:0-DHSM, or DPPC were characterized using steady-state and time-resolved fluorescence spectroscopy and different fluorescent reporter molecules. The acyl-chain region was probed using free and phospholipid-bound 1,6-diphenyl-1,3,5-hexatriene. 16:0-DHSM was found to be the more ordered than both DPPC and 16:0-SM 5°C below and above melting temperature. Interfacial properties of the phospholipid bilayers were examined using 6-dodecanoyl-2-dimethyl-aminonaphthalene (Laurdan), 6-propionyl-2-dimethyl-amino-naphthalene (Prodan), and dansyl-PE. Laurdan and Prodan reported that the two sphingomyelin (SM) membrane interfaces were clearly different from the DPPC membrane interface, whereas the two SM membrane interfaces had more similar properties (both in gel and liquid-crystalline phase). Prodan partition studies showed that membrane resistance to Prodan partitioning increased in the order: 16:0-SM < DPPC < 16:0-DHSM. The degree to which dansyl-PE is exposed to water reflects the structural properties of the membrane-water interface. By comparing the lifetime of dansyl-PE in water and deuterium oxide solution, we could show that the degree to which the dansyl moiety was exposed to water in the membranes increased in the order: 16:0-SM < DPPC < 16:0-DHSM. In conclusion, this study has shown that DHSM forms more ordered bilayers than acyl-chain matched SM or phosphatidylcholine, even in the liquid-crystalline state.

INTRODUCTION

Mammalian cell membranes are composed of a complex array of various glycerophospholipids, sphingolipids, and cholesterol. Variations in headgroup and acyl-chain composition among sphingo- and glycerophospholipids add an additional level of complexity to membrane composition. Sphingomyelin (SM) is the major sphingolipid class present in the external leaflet of cellular plasma membranes. Although both SM and phosphatidylcholine (PC) contain phosphocholine as the polar headgroup, their hydrophobic backbone is different. This leads to differences in the interfacial properties resulting from hydrogen bonding differences, inasmuch as SM contains both hydrogen bond donating and accepting groups, whereas PC only has hydrogen bond accepting groups. Because of these properties it is thought that SMs have stronger intermolecular interactions between neighboring molecules and with cholesterol than PCs (Slotte, 1999; Ohvo-Rekila et al., 2002). It has been suggested that the favorable interactions between SM and cholesterol gives rise to cholesterol and SM rich domains or rafts. The rafts are believed to be important in protein and lipid transport and sorting, as well as in several signaling cascades (Simons and Ikonen, 1997). The nature of the interactions between SM and cholesterol remains unclear. However, it seems that the interactions are stabilized by hydrogen bonding (Sankaram and Thompson, 1990; Bittman et al., 1994; Veiga et al., 2001).

Most of the naturally occurring SMs have the phosphocholine headgroup linked to the hydroxyl group on carbon 1 of a long-chain base (most often an 18-carbon amine diol), and have a long and highly saturated acyl chain linked to the amide group on carbon 2 of the long-chain base (for a review, see Barenholz, 1984). These SMs have the D-*erythro*-(2S,3R) configuration of the long-chain base (Sarmientos et al., 1985). In cultured cells (i.e., human skin fibroblast and baby hamster kidney cells) ~90–95% of the SMs contain sphingosine (1,3-dihydroxy-2-amino-4-octadecene) as the long-chain base, whereas the remainder have sphinganine (1,3-dihydroxy-2-amino-4-octadecane) as the base (Ramstedt et al., 1999). The latter SMs are also called dihydrosphingomyelins (DHSM). Although it is currently not known why cells need both SMs and DHSMs, it is remarkable that DHSM accounts for 50% of all phospholipids in human lens membranes (Byrdwell and Borchman, 1997).

The physico-chemical properties of DHSM are not nearly as well documented as those of SM, but it is known that the lack of the *trans* double bond between carbons 4 and 5 in

DHSM leads to a higher melting temperature (T_m) compared to acyl-chain matched SM (Barenholz et al., 1976). As a consequence, DHSMs are even more likely than SM to undergo lateral phase separation in bilayer membranes, and may thus contribute to the formation of laterally condensed domains in biomembranes (Brown, 1998; Kuikka et al., 2001). The sphingolipid and cholesterol-rich lipid rafts of cell membranes are known to be resistant to Triton X-100 induced solubilization at low temperatures (Brown and Rose, 1992; Schroeder et al., 1994; London and Brown, 2000). In model membrane systems, we have shown that Triton X-100 partitioning into unilamellar vesicles containing 16:0-SM was described by a lower partition coefficient, and a lower Gibbs free energy as compared to vesicles prepared from DPPC (Nyholm and Slotte, 2001). Partitioning of detergents into vesicles prepared from egg DHSM was also accompanied by lower partition coefficients and lower Gibbs free energies as compared to studies on vesicles made from egg SM (Ollila and Slotte, 2002).

In the present work, we have chosen to characterize both the interfacial properties and the dynamics of the bulk membrane interior of bilayer vesicles containing either D-*erythro*-N-palmitoyl-sphingomyelin, D-*erythro*-N-palmitoyl-dihydrosphingomyelin, or 1,2-dipalmitoyl-*sn*-glycero-3-phosphocholine. The interfacial properties of the bilayer membranes were studied by measuring the spectral shifts of Laurdan and Prodan (Weber and Farris, 1979; Massey and Pownall, 1998; Krasnowska et al., 1998), and by determining the fluorescence lifetime and deuterium isotope exchange of dansyl-phosphatidylethanolamine (Abbott and Nelsestuen, 1987; Epand and Leon, 1992; Asuncion-Punzalan et al., 1998). Information about order in the bulk hydrophobic core of the vesicle membranes was derived from steady-state and time-resolved fluorescence measurements of free and phospholipid-bound diphenylhexatriene (Parente and Lentz, 1985; Williams and Stubbs, 1988; Kalb et al., 1989; Lentz, 1989).

EXPERIMENTAL PROCEDURES

Materials

16:0-SM was purified from egg yolk SM (Avanti Polar Lipids, Alabaster, AL, USA) by reverse-phase high-performance liquid chromatography (LiChrospher 100 RP-18 column, 5 μm particle size, 240 × 4 mm column dimension) using 5 vol % water in methanol as the eluent (at 1 ml/min, column temperature 40°C). The purity and the proper composition of the 16:0-SM (as well as all the other phospholipids) were verified by mass spectrometry. D-*erythro*-N-palmitoyl-dihydrosphingomyelin (16:0-DHSM) was prepared from 16:0-SM by hydrogenation using palladium oxide (Aldrich Chemical, Milwaukee, WI, USA) as the catalyst (Schneider and Kennedy, 1967), and purified as described for 16:0-SM. DPPC was purchased from Avanti Polar Lipids. DPH, DPH-PC, DPH propionic acid, Laurdan, Prodan, and dansyl-PE were obtained from Molecular Probes (Leiden, the Netherlands). Deuterium oxide (D_2O) was obtained from Aldrich Chemical.

DPH-SM was prepared from D-*erythro*-lysosphingomyelin (Avanti Polar Lipids) and DPH propionic acid as previously described (Cohen et al., 1984; Ramstedt and Slotte, 1999). The DPH-SM formed was initially purified using bonded phase columns according to Kaluzny and co-workers (Kaluzny et al., 1985), followed by reversed phase chromatography on a LiChrospher 100 RP-18 column (5 μm particle size, 250 × 4 mm column dimensions) using methanol at a flow of 1 ml/min. DPH-DHSM was produced from D-*erythro*-lysodihydrosphingomyelin and DPH propionic acid as described for DPH-SM. The hydrogenation of D-*erythro*-lyso-sphingomyelin was performed as described for 16:0-SM above. Stock solutions of lipids were prepared in hexane:2-propanol (3:2, v/v), stored in the dark at −20°C, and warmed to ambient temperature before use.

Lipid vesicles were prepared in Dulbecco's phosphate buffered saline. In short, the dry lipids and fluorophore were rehydrated at 60°C in phosphate buffered saline (saturated with argon) and sonicated in a Bransonic 2510 (Branson Ultrasonics, CT, USA) bath sonicator for 20 min at 60°C. To protect the fluorophores, the sonication was performed in darkness and in an argon atmosphere. The concentrations of all fluorescent probe solutions were determined from the molar extinction coefficients as provided by Molecular Probes. For DPH-DHSM and DPH-SM solutions, we used the molar extinction coefficients of DPH-PC.

Steady state fluorescence measurements

All steady-state fluorescence experiments presented in this paper were performed on a PTI QuantaMaster 1 (Photon Technology International, Lawrenceville, NJ, USA) spectrofluorimeter operating in the T-format, with both the excitation and emission slits set to 5 nm (unless otherwise specified). The temperature was controlled by a Peltier element, with a temperature probe immersed in the sample solution. All experiments were made in quartz cuvettes and the sample solutions were kept at constant stirring (260 rpm) throughout the measurements. Background fluorescence was measured using the corresponding lipid solutions without fluorophores, and subtracted from the sample spectra. All emission spectra have been corrected to compensate for the wavelength dependence of the detector.

Steady-state fluorescence anisotropy

Steady-state fluorescence anisotropy of DPH-labeled phospholipids was determined in vesicles containing either DPPC, 16:0-SM, or 16:0-DHSM (50 μM) and 1 mol % of DPH-PC, DPH-SM, or DPH-DHSM, respectively. The vesicles were prepared by bath sonication as described above. DPH-labeled phospholipids were included with the bulk lipid before sonication. Excitation was carried out at 360 nm and the emission was recorded at 430 as the temperature was scanned between 20 and 60°C. The steady-state anisotropy, r, is defined as:

$$r = (I_\parallel - GI_\perp)/(I_\parallel + 2GI_\perp),$$

where $I_\parallel$ and $I_\perp$ are the fluorescence intensities with the analyzer parallel and perpendicular, respectively, to the vertical polarizer, and G represents the ratio of the sensitivity of the system for vertically and horizontally polarized light (Lakowicz, 1999).

Laurdan emission spectra

Laurdan emission spectra were recorded at 5°C below and above the gel-liquid phase transition of DPPC (36 and 46°C, respectively), 16:0-SM (36 and 46°C) and 16:0-DHSM (43 and 53°C). The total lipid concentration in the cuvette was 100 μM, out of which 1 mol % was Laurdan. Laurdan was included with the lipids before hydration and bath sonication (60°C) of the hydrated lipids. The emission spectra were collected between 390 and 550 nm, whereas the sample was excited at 360 nm. All spectra were recorded as the average of three scans.

Prodan emission spectra

Emission spectra of Prodan were measured in 50 μM phospholipid solutions containing 1 mol % Prodan. Excitation was performed at 360 nm and the emission intensity was recorded between 390 and 590 nm. Vesicles were produced with bath sonication at 60°C. Prodan was added from an ethanolic stock solution (1.7 mM) to the preformed vesicles and the solution was allowed to equilibrate (10 min at 25°C) before the emission spectra were measured at 5°C on both sides of T_m for the bulk phospholipids in the vesicles.

Time-resolved fluorescence measurements

All time-resolved fluorescence measurements were performed on a PTI TimeMaster (Photon Technology International) instrument. The light source in these experiments was an N_2 laser. Data analysis was performed with the software (TimeMaster 1.2) supplied by the instrument manufacturers. Goodness of fit was determined from the reduced Chi^2, Durbin-Watson, z value, and the weighted residuals.

Lifetimes of free and phospholipid-bound DPH in bilayer membranes

For these experiments, phospholipid vesicles contained either DPPC, 16:0-SM, or 16:0-DHSM (50 μM) and 0.33 mol % of either DPH-PC, DPH-SM, or DPH-DHSM, respectively. When free DPH was included, it was added to 1 mol %. The samples were excited at 337 nm, which is the wavelength generated by the N_2 laser, and the emission was measured at 430 nm. The slits were set to 8 nm (except with samples containing free DPH when 12 nm was used). Time-resolved anisotropies were calculated using the following equation

$$r(t) = \sum_i r_{0i} \exp(-t/\phi_i),$$

where r_{0i} are the fractional anisotropies that decay with correlation times ϕ_i. The order parameter, S, and the cone angle, θ_C, were calculated from the fundamental anisotropy, r_0, and the limiting anisotropy r_∞ (Lakowicz, 1999).

$$\left(\frac{r_\infty}{r_0}\right)^{(1/2)} = S = \frac{1}{2}\cos\theta_c(1 + \cos\theta_c)$$

Dansyl-phosphatidylethanolamine fluorescence lifetimes in phospholipid membranes

Fluorescence lifetimes of dansyl-PE were measured in vesicles containing one of the three phospholipids together with 1 mol % dansyl-PE (total lipid concentration 50 μM). The samples were excited at 337 nm and emission was measured at 516 nm with a slit width of 8 nm. Dansyl-PE emission lifetimes were measured in buffer prepared either in water (H_2O) or D_2O.

Time-resolved fluorescence of Prodan in phospholipid membranes

Emission lifetimes of Prodan were measured in sonicated vesicles containing 0.33 mol % Prodan (150 μM total lipid concentration). The vesicles were prepared as previously described. The excitation wavelength was set to 360 nm. This wavelength was achieved with a dye laser, containing BPBD-365 (Exciton, Dayton, Ohio, USA) as the laser dye. The emission monochromator was removed and the emission was recorded through a 400CFLP (Melles Griot, Zevenaar, The Netherlands) cut-off filter. To minimize the amount of scattered light reaching the detector the emitted light was also filtered through a polarizer set at a 90° angle relative to the excitation light.

The partition coefficient (C_p) of Prodan between bilayer and water was calculated using a method described by Krasnowska and co-workers (Krasnowska et al., 1998, 2001), where C_p is calculated according to

$$C_p = R_M \frac{[W]}{[Lipids]},$$

where $[W]$ is the molar concentration of water (55.5 M) and $[Lipids]$ is the total lipid concentration. R_M describes the ratio of Prodan in water and membrane, and is calculated from the following equation:

$$R_M = R_F \frac{\tau_W}{\tau_M}.$$

Here it is assumed that the lifetime is proportional to the quantum yield, which allows the use of the lifetime of Prodan in water (τ_W) and membrane (τ_M) in the calculation of R_M. R_F is the ratio between Prodan fluorescence arising from the membrane and from the aqueous phase. R_F is calculated according to

$$R_F = \frac{F_M}{F_W},$$

where F_M and F_W are the fractional intensities of Prodan fluorescence in membrane and in water, respectively.

RESULTS

Steady-state anisotropy of phospholipid-bound DPH in vesicle membranes

The functional role of SMs in natural cell membranes seems to be different from that of glycerophospholipids. Because SMs (and other sphingolipids) have more saturated acyl chains and have more hydrogen-bonding capabilities as compared to glycerophospholipids, they are probably better suited to function as structural components of membrane rafts. DHSMs are even more saturated and are known to form lateral domains in model membrane systems (Kuikka et al., 2001). In this study we have done a thorough examination of the interfacial and dynamic properties of acyl-chain defined SMs together with an acyl-chain matched phosphatidylcholine.

The steady-state anisotropy (r_{ss}) of DPH-PC, DPH-SM, and DPH-DHSM was recorded as a function of temperature in DPPC, 16:0-SM, and 16:0-DHSM vesicles, respectively. In all three vesicle types the gel to liquid-crystalline phase transition was clearly reported by a rapidly decreasing anisotropy of the DPH-labeled phospholipids close to the transition temperature of the bulk vesicle phospholipids. In the gel phase (between 20 and ~32°C), the r_{ss} was highest for DPH-PC in DPPC, followed by DPH-DHSM in 16:0-DHSM and DPH-SM in 16:0-SM. Although all three bulk lipids have been shown to go through a pretransition when warmed from their gel phase to their liquid phase (McMullen et al., 1993; Kuikka et al., 2001), only DPH-DHSM in 16:0-DHSM vesicles appeared to report this transition, as evidenced by the increased r_{ss} before the main transition (Fig. 1).
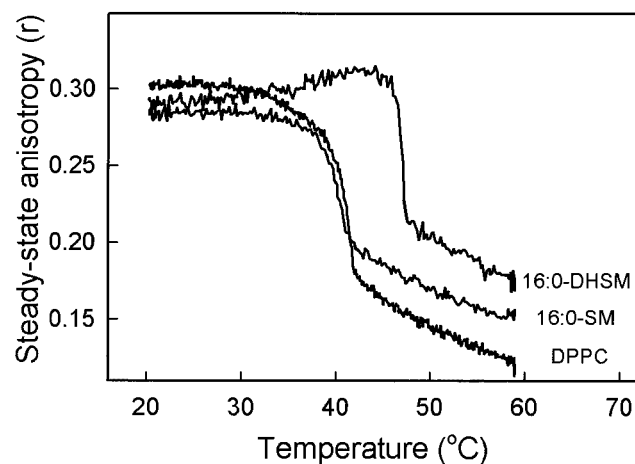
FIGURE 1 Steady-state anisotropy (r_{ss}) of phospholipid-bound DPH in phospholipid bilayers as a function of temperature. The measurements were performed on DPH-SM, DPH-DHSM, and DPH-PC in 16:0-SM, 16:0-DHSM, and DPPC, respectively. All curves shown in the graph are an average curve of three separate experiments.

## Intensity decay of free and phospholipid-bound DPH in membranes

The effect of the bilayer environment on the fluorescence lifetimes of free DPH, or covalently attached DPH (i.e., DPH-PC, DPH-SM, and DPH-DHSM) was determined for DPPC, 16:0-SM, and 16:0-DHSM vesicle membranes at ~5°C below and above the T_m of the bulk lipid. The results from the experiments with free DPH are summarized in Table 1. In the analysis, the best fits were gained with a model containing two exponential decays, a shorter component with decay time of ~2.9 ns (τ_2), and a longer component with a more varied decay time (τ_1). As the temperature was raised above the phase transition temperature, τ_1 got shorter due to the decreased packing density in the liquid-crystalline phase, whereas the τ_2 component tended to increase slightly after the transition. Below the phase transition, where the phospholipid membranes were in the gel phase, τ_1 was longer and appeared to be more sensitive to the composition of the membrane than in the liquid-crystalline phase. τ_1 for
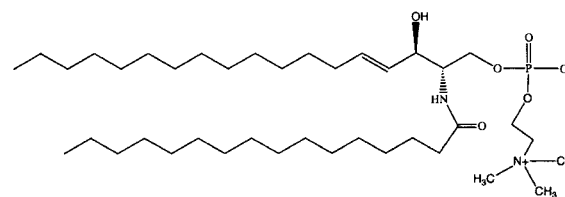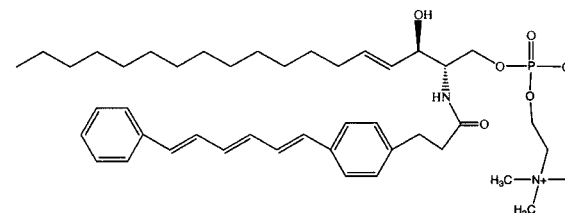

D-*erythro*-N-16:0-sphingomyelin (2S,3R)
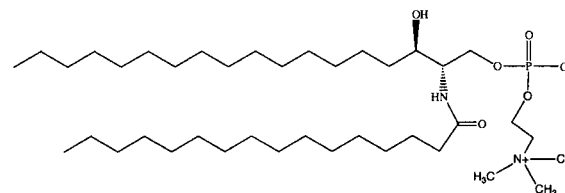
D-*erythro*-N-16:0-dihydrosphingomyelin (2S,3R)
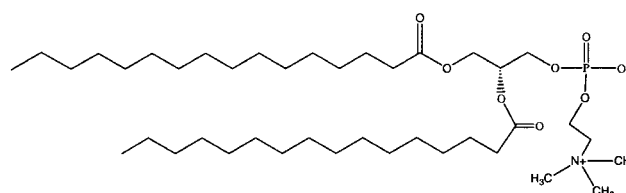
1,2-dipalmitoyl-sn-glycero-3-phosphocholine

D-*erythro*-N-DPH-sphingomyelin (2S,3R)

SCHEME 1 A schematic representation of the phospholipids used in this study.

TABLE 1 Fluorescence-decay parameters of free DPH in DPPC, 16:0-SM, and 16:0-DHSM membranes at 5°C above and below T_m

Bulk lipid	T (°C)	Pre-exp. factor		Fractional intensity		Lifetime (ns)		Chi^2
		α_1	α_2	f_1	f_2	τ_1	τ_2	
DPPC	36	0.819	0.181	0.945	0.055	9.79	2.57	0.817
DPPC	46	0.829	0.171	0.926	0.074	8.43	3.28	0.952
16:0-SM	36	0.792	0.208	0.947	0.053	11.17	2.39	0.850
16:0-SM	46	0.792	0.208	0.933	0.067	8.93	2.43	0.817
16:0-DHSM	43	0.900	0.100	0.971	0.029	10.67	2.86	0.918
16:0-DHSM	53	0.721	0.279	0.868	0.132	9.46	3.71	1.070

All data in this table are the averages of at least three separate experiments. The standard deviations were below 5% for τ_1, whereas the value of τ_2 varied more.

DPH in DPPC membranes was markedly shorter than τ_1 for DPH in 16:0-SM or 16:0-DHSM membranes. To determine whether a higher degree of H_2O access to DPH in DPPC membranes shortened the lifetime, we performed corresponding experiments in D_2O (results not shown). Because changing the solvent to D_2O had no significant effect on the fluorescence lifetime of free DPH in any of the membrane types (above or below T_m), other factors than water probably induced the shortening of the τ_1 in DPPC membranes as compared to in SM membranes.

With phospholipid-bound DPH, the fluorescence lifetimes of the DPH moiety again showed two lifetime components (Table 2). With phospholipid-bound DPH, both lifetime components (τ_1 and τ_2) decreased as the bulk lipid went from a gel phase to a liquid-crystalline phase. The τ_2 was shorter for all three lipid environments when the DPH was phospholipid-linked as compared with situation of the free probe. The differences in lifetimes among the three different phospholipid-bound DPH probes were much smaller when compared to free DPH. To study whether water affected the lifetime of phospholipid-bound DPH in the different membrane types, we performed corresponding experiments in D_2O solution. The phospholipid-bound DPH lifetimes were similar in all membrane types irrespective of whether the membranes were hydrated with D_2O or H_2O (data not shown).

Time-resolved anisotropy of phospholipid-bound DPH in membranes

To get more information about the molecular order and dynamics of the three phospholipids, we also measured the time-resolved anisotropies of DPH phospholipids in the different vesicles. In these experiments, the fluorescence intensity decays were best represented by a biexponential fit, with similar decay times as presented above. The anisotropy decay of each system was best represented by a single exponential decay. The results from these measurements are shown in Table 3, and include the values of the rotational correlation time (ϕ), the order parameter (S), the residual anisotropy (r_∞), and the cone angle (θ_C). Measurements were

TABLE 3 Anisotropy decays of DPH-DPPC in DPPC membranes, DPH-16:0-SM in 16:0-SM membranes, and DPH-16:0-DHSM in 16:0-DHSM membranes at 5°C above and below T_m

Bulk lipid	Temp. (°C)	ϕ (ns)	S	r_∞	θ_C (degrees)
DPPC	36	3.21 ± 0.20	0.84 ± 0.02	0.28 ± 0.02	27.34 ± 1.97
DPPC	46	3.00 ± 0.05	0.53 ± 0.02	0.11 ± 0.01	50.28 ± 1.52
16:0-SM	36	3.79 ± 0.14	0.81 ± 0.01	0.25 ± 0.01	31.83 ± 2.53
16:0-SM	46	3.62 ± 0.13	0.47 ± 0.04	0.08 ± 0.01	55.33 ± 2.52
16:0-DHSM	43	3.07 ± 0.09	0.91 ± 0.03	0.32 ± 0.02	22.27 ± 0.32
16:0-DHSM	53	3.05 ± 0.15	0.64 ± 0.01	0.16 ± 0.01	42.43 ± 0.79

All data in this table are the averages of at least three separate experiments $\pm$ SD. The cone angle (θ_C) was calculated assuming that the rotation of the DPH-phospholipid molecules was energetically impossible beyond a certain angle.

performed 5°C below and above the T_m of the bulk lipid. Raising the temperature above the phase transition temperature of the bulk phospholipids led to decreased order and restriction of molecular motions, as seen from the increased cone angle and decreased order parameter. Of the phospholipids studied, 16:0-DHSM was the most ordered, both in the gel and the liquid-crystalline phase. DPPC bilayers appeared to be slightly more ordered than the 16:0-SM bilayers, both above and below the phase transition.

Lifetime of dansyl-PE fluorescence in membranes

The fluorescence lifetime and deuterium isotope exchange of dansyl-PE was used to study the exposure of the probe to water in the bilayer headgroup region. The dansyl moiety of the fluorescent probe is located at the water/lipid interface (Abbott and Nelsestuen, 1987; Asuncion-Punzalan et al., 1998), and its lifetime is primarily sensitive to the local environment, to which the major contribution comes from water (Epand and Leon, 1992). In addition, fluorophores with an exchangeable hydrogen, such as dansyl, are known to have a greater quantum yield in D_2O relative to H_2O due to a reduced rate of proton transfer (Stryer, 1966). An increase in the lifetime of dansyl-PE in D_2O compared to in

TABLE 2 Fluorescence-decay parameters of DPH-DPPC in DPPC membranes, DPH-16:0-SM in 16:0-SM membranes, and DPH-16:0-DHSM in 16:0-DHSM membranes at 5°C above and below T_m

Bulk lipid	T (°C)	Pre-exp. factor		Fractional intensity		Lifetime (ns)		Chi^2
		α_1	α_2	f_1	f_2	τ_1	τ_2	
DPPC	36	0.676	0.324	0.818	0.182	7.39	3.44	0.967
DPPC	46	0.829	0.171	0.949	0.051	6.49	1.69	0.860
16:0-SM	36	0.605	0.395	0.835	0.165	7.10	2.16	0.983
16:0-SM	46	0.582	0.418	0.863	0.137	6.40	1.41	0.773
16:0-DHSM	43	0.744	0.256	0.891	0.109	7.76	2.76	1.004
16:0-DHSM	53	0.873	0.127	0.945	0.055	7.47	2.98	0.947

All data in this table are the averages of at least three separate experiments. The standard deviations were below 5% for τ_1, whereas the value of τ_2 varied more.

H_2O therefore indicates exposure to water. Hence, the D_2O/H_2O lifetime ratio reflects the properties in the headgroup region of membranes (Ho et al., 1995; Ho and Stubbs, 1997; Saito et al., 2000). All intensity decays recorded with dansyl-PE were best represented by a single exponential fit (data not shown). The D_2O/H_2O lifetime ratios (Table 4) were all larger than 1, indicating that dansyl-PE was exposed to water in all membrane types. The D_2O/H_2O lifetime ratio increased as the bulk lipid went from gel phase to liquid-crystalline phase, which is expected inasmuch as the degree of hydration is known to increase as the bilayer melts (Kinnunen, 1991). The change in D_2O/H_2O lifetime ratio when going from gel to liquid-crystalline phase was similar for DPPC and 16:0-SM, but was smallest for 16:0-DHSM, indicating that the amount of water in the vicinity of the dansyl group was not changed markedly in 16:0-DHSM membrane upon phase transition.
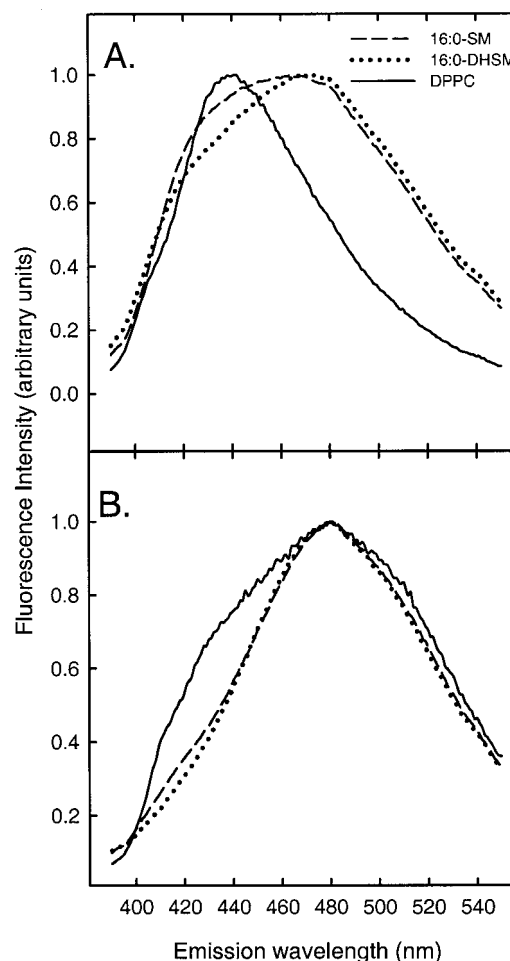
Emission spectra of Laurdan in membranes

To probe for polarity differences at the aqueous/vesicle interface of the three different phospholipid membranes, we recorded Laurdan emission spectra at 5°C below and above the respective transition temperature of the vesicles. Representative emission spectra of Laurdan in 16:0-SM, 16:0-DHSM, and DPPC vesicles are shown in Fig. 2. At $T_m - 5°C$ (Fig. 2 A), Laurdan in the DPPC vesicles gave a very blue-shifted emission band, whereas the two SMs had more red-shifted emission bands, the 16:0-SM band being broader than the corresponding 16:0-DHSM band. In the liquid-crystalline phase ($T_m + 5°C$), the emission spectra of Laurdan in 16:0-SM and 16:0-DHSM vesicles were identical whereas that in DPPC differed by being broader than the SM bands (Fig. 2 B). Clearly the SM interfaces were more polar than the DPPC interface at temperatures below the main transition, and even above the transition, DPPC vesicles displayed more Laurdan emission intensity from a less polar environment compared to both SMs. It is possible that the difference in hydrogen-bonded network in sphingomyelin membranes affected the depth to which Laurdan penetrated the membrane, and hence in this respect affected the environment around the probe.

TABLE 4   Fluorescence decay of dansyl-PE in DPPC; 16:0-SM or 16:0-DHSM vesicles prepared in H_2O and D_2O solutions at 5°C above and below T_m

Bulk lipid	Temp. (°C)	τ (H_2O)	τ (D_2O)	τ (D_2O)/τ (H_2O)
DPPC	36	15.01 ± 0.13	16.35 ± 0.21	1.09
DPPC	46	13.24 ± 0.23	15.01 ± 0.21	1.13
16:0-SM	36	17.42 ± 0.68	18.37 ± 0.52	1.05
16:0-SM	46	15.82 ± 0.37	17.19 ± 0.39	1.09
16:0-DHSM	43	16.54 ± 0.80	18.45 ± 0.38	1.12
16:0-DHSM	53	14.85 ± 0.83	16.97 ± 0.04	1.14

The decay times are the average value of at least three separate experiments $\pm$ SD. The τ (D_2O)/τ (H_2O) ratios were calculated from the average lifetimes.

FIGURE 2   Emission spectra of Laurdan in DPPC, 16:0-SM, and 16:0-DHSM bilayers at $T_m - 5°C$ (A) and $T_m + 5°C$ (B). All emission spectra in the graph were background subtracted, corrected, and normalized.

Prodan partitioning into membranes

Information of Prodan partitioning into DPPC, 16:0-SM, and 16:0-DHSM vesicles was obtained from both steady-state emission spectra and measurements of lifetimes of the emitted light. The emission spectra of Prodan in DPPC, 16:0-SM, and 16:0-DHSM vesicles were measured 5°C below and above the phase transition temperature. In the gel phase (Fig. 3 A), the spectra showed two distinct bands. The blue emission band originated from Prodan located in the membrane, whereas the red emission band derived from Prodan in water (Krasnowska et al., 1998, 2001). Thus, the relative intensities in the two bands describe the degree to which Prodan partitioned into the membrane. The highest intensity from Prodan in the membrane (blue emission) was seen with 16:0-SM vesicles, whereas the blue emission was markedly reduced for 16:0-DHSM membranes. For DPPC membranes, the blue emission signal was intermediate to the two SMs, and was slightly less blue shifted, indicative of a more polar surrounding in the DPPC membrane compared
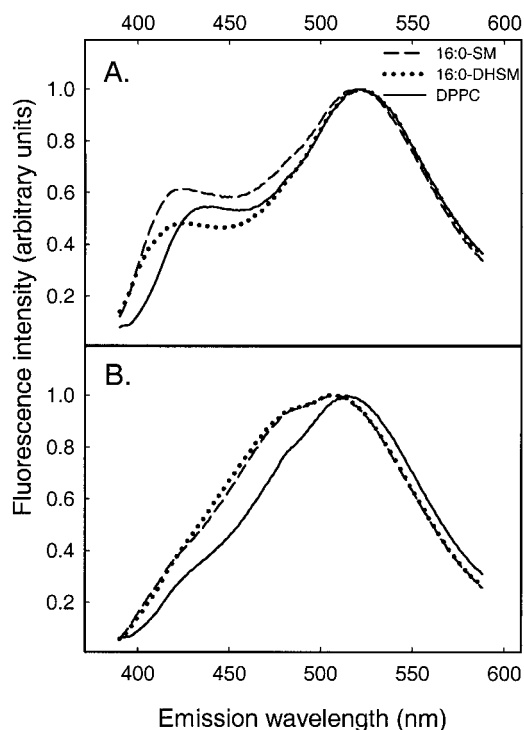
FIGURE 3 Emission spectra of Prodan in DPPC, 16:0-SM, and 16:0-DHSM bilayers at $T_m - 5°C$ (A) and $T_m + 5°C$ (B). All emission spectra in the graph were background subtracted, corrected, and normalized.

TABLE 5 Prodan partitioning into bilayers of different phospholipid composition

| Bulk lipid | T (°C) | Lifetime (ns) | | $C_p \times 10^4$ |
		τ_1	τ_2	
DPPC	36	4.7 ± 0.3	1.1 ± 0.1	4.24 ± 0.15
DPPC	46	3.3 ± 0.1	1.0 ± 0.1	5.57 ± 0.57
16:0-SM	36	4.2 ± 0.1	1.0 ± 0.1	4.60 ± 0.50
16:0-SM	46	3.4 ± 0.1	1.0 ± 0.1	5.81 ± 0.76
16:0-DHSM	43	3.8 ± 0.1	1.0 ± 0.1	3.18 ± 0.21
16:0-DHSM	53	3.4 ± 0.2	1.0 ± 0.1	3.69 ± 1.00

Phospholipid vesicles were prepared by bath sonication, and 0.33 mol % Prodan was added at 25°C. The partition coefficient (C_p) was calculated as described under the Experimental procedures. All data in this table are the averages of at least three separate experiments ± SD.

to the two SM membranes. In the liquid-crystalline phase (5°C above the transition temperature; Fig. 3 B), the emission spectra of Prodan in 16:0-SM and 16:0-DHSM vesicles were superimposable, whereas the emission band from DPPC membranes was more red shifted.

Time-resolved measurements of Prodan emission showed that the intensity decays were described by two lifetimes components. The shorter lifetime originated from Prodan in water whereas the longer component represented intensity decay of Prodan in a membrane environment (Krasnowska et al., 1998, 2001). The two measured lifetime components were used to calculate the partition coefficient (C_p) of Prodan partitioning between phospholipid membranes and bulk water. As expected, Prodan partitioned more efficiently into liquid-crystalline membranes than in gel phase membranes (Table 5). When the three phospholipids were compared, it was observed that Prodan partitioned best into 16:0-SM vesicles. 16:0-DHSM membranes were most resistant to Prodan partitioning, whereas DPPC vesicles had intermediate C_p:s.

DISCUSSION

It has previously been shown that DHSMs differ from acyl-chain matched SMs by having higher melting temperatures and lower crystallization pressures in monolayers (Kuikka

et al., 2001). These observations indicate that there are stronger cohesive forces between DHSMs than between SMs in the model membranes, probably largely due to better lateral packing of DHSMs. The finding that DHSM molecules are brought closer to each other compared to SM molecules have been shown to affect the hydrogen bond network in the headgroup region of membranes composed of DHSMs (Ferguson-Yankey et al., 2000; Talbott et al., 2000). The conclusions from the aforementioned studies were that SMs form more stable intramolecular hydrogen bonds than DHSMs, whereas DHSMs tend to form more stable intermolecular hydrogen bonds. The aim of this study was to obtain more information about the membrane properties of DHSMs to deepen the understanding of their role in cellular membranes, and especially in the membranes of human eye lens cells.

Steady-state and time-resolved fluorescence emission from free and phospholipid-bound DPH

DPPC and 16:0-SM have almost the same phase transition temperature, whereas 16:0-DHSM has a phase transition temperature that is ~7°C higher (Small, 1986; Kuikka et al., 2001). The properties of phospholipid membranes are to a high degree governed by how the experimental temperature is related to the phase transition temperature. Therefore, we chose to study the properties of the phospholipid bilayers at 5°C on both sides of the phase transition. Hence, the phospholipid membranes were studied both in the gel phase and in the liquid-crystalline phase. The hydrophobic core region of the bilayers was studied by means of two fluorescent probes; free DPH and phospholipid-bound DPH, of which free DPH has been shown to locate slightly closer to surface of the membrane (Kaiser and London, 1998). The lifetime of DPH is extremely sensitive to the dielectric constant of the medium (Fiorini et al., 1987). The extent to which water is allowed to penetrate the membrane is known to affect the lifetime of DPH (Shinitzky and Barenholz, 1978; Barrow and Lentz, 1985; Lentz, 1989; Pap

et al., 1994; Bernsdorff et al., 1997). The lifetime of free DPH in DPPC vesicles was shorter in comparison to SM and DHSM membranes (below the phase transition). Because the lifetimes of DPH were similar irrespective of whether the vesicles were in a D_2O- or H_2O-based solution, it seems that water does not affect the lifetime of DPH. Rather some other membrane property seems to be involved. It was also observed that free DPH had a shorter lifetime in 16:0-DHSM vesicles than in 16:0-SM membranes.

Linking DPH to phospholipids leads to fluorescent probes with different properties than free DPH. For instance, free DPH have been shown to be homogeneously distributed in membranes, whereas the phosphatidylcholine-bound derivative has been shown to partition preferentially into loosely packed membrane regions (Lentz et al., 1976; Andrich and Vanderkooi, 1976; Parente and Lentz, 1985). Similarly the DHSM- and SM-bound DPH has been observed to partition preferentially in fluid membrane regions (unpublished observation; Nyholm and Slotte, 2002). Because the fluorophore replaced an acyl chain in DPPC, 16:0-SM, and 16:0-DHSM, the DPH moiety should have a more defined position in the membrane than the free DPH. Therefore it seems reasonable that these probes should be good reporters of the acyl chain dynamics in these respective bilayer compositions. When phospholipid-bound DPH was used as a reporter molecule in phospholipid bilayers in the gel phase, the lifetimes of DPH in DPPC, 16:0-SM, and 16:0-DHSM were different in relation to those obtained with free DPH. Again we assessed the water access to the probe the different membrane types by comparing the lifetimes measured in H_2O- and D_2O-based solutions. Inasmuch as phospholipid-bound DPH proved to have similar lifetimes in H_2O and D_2O in all membranes types, the differences in lifetime could be due to other factors than the presence of various degrees of water.

The amount of *cis* double bonds in the acyl chains of phospholipids is known to have dramatic effects on the order and dynamics of the membrane. How the *trans* double bond that is present in the sphingoid base of most natural SMs affects the membrane dynamics has not been that extensively studied. Here we addressed this question by studying the dynamics of phospholipid-bound DPH in 16:0-SM and 16:0-DHSM vesicles. Previous studies have indicated that DHSMs pack more tightly, and have stronger intermolecular interactions than SMs (Talbott et al., 2000; Kuikka et al., 2001). Therefore, it was not surprising that DPH-DHSM in 16:0-DHSM membranes was less mobile than the DPH-SM in 16:0-SM membranes, as seen from the anisotropy decays of the reporter molecules. DPPC, like 16:0-DHSM, is fully saturated, but still DPPC membranes were not as ordered as 16:0-DHSM membranes, and had T_m:s ~7 degrees lower than the acyl-chain matched 16:0-DHSM. This could be due to tighter lateral packing of 16:0-DHSM than of DPPC, but also to differences in hydrogen bonding in the two membrane types.

The water exposure of dansyl-phosphatidylethanolamine in the membrane-water interface

To evaluate the role of water in the membrane-water interface, dansyl-PE was included into the phospholipid vesicles. The dansyl moiety of dansyl-PE has been shown to localize within the headgroup region of the bilayer (Asuncion-Punzalan et al., 1998). Hence, the results contain structural information of the phosphocholine headgroups in DPPC, 16:0-SM, and 16:0-DHSM. The same method was used by Saito and co-workers to study how the inclusion of egg yolk SM and DPPC alters the membrane surface structure of egg yolk phosphatidylcholine-triolein emulsions (Saito et al., 2000). They showed that the dansyl moiety was less accessible to water when SM was included in the emulsions than when DPPC was included. They concluded that this probably was an effect of the inter- and intra-molecular interactions that are believed to be formed by SMs but not by phosphatidylcholines. Similar conclusions were made by Jendrasiak and Smith (2001), who studied the hydration of SM and phosphatidylcholine monolayers. In our work we found that the degree to which the dansyl group was exposed to water in the three systems studied increased in the order: 16:0-SM < DPPC < 16:0-DHSM. We also found that dansyl-PE had a shorter fluorescence lifetime in DPPC vesicles than in the SM vesicles, which is in agreement with a previous report (Saito et al., 2000). The mechanism for this remains unclear. However, it emphasizes the differences in interfacial properties between SM and PC membranes.

Interfacial differences as revealed by Laurdan emission spectra

In monolayers studies, it has previously been shown that DHSMs had a 100 mV lower surface potential than acyl-chain matched SMs (Kuikka et al., 2001). Data from NMR spectroscopy again indicates that DHSMs and SMs interact differently with water molecules (Talbott et al., 2000). To obtain more information of the properties of the headgroup region of bilayers composed of DHSMs, SMs, and phosphatidylcholines, we measured emission spectra of Laurdan in the different phospholipid environments. The amino-naphtalene-carbonyl fluorescent moiety of Laurdan renders it particularly sensitive to the polarity of the environment (Weber and Farris, 1979; Massey and Pownall, 1998; Krasnowska et al., 1998). In phospholipid membranes, Laurdan monitors relevant differences in the polarity and the different phase states (Zeng and Chong, 1991; Rottenberg, 1992; Parasassi et al., 1994, 1997).

Excitation and emission spectra of Laurdan in DPPC and different SM membranes have already been presented in a number of studies (Bagatolli et al., 1997, 1998, 1999; Massey, 2001). The SMs that have been used in these studies

have been natural SMs like egg yolk or bovine brain SM, which contain SMs with several different acyl-chain lengths. In the present study, only D-*erythro*-*N*-16:0-DHSM or D-*erythro*-*N*-16:0-SM has been used, resulting in a more homogenous system from which the signal is measured. In the gel phase, Laurdan had broader emission spectra in 16:0-SM and 16:0-DHSM membranes than in DPPC membranes. This could indicate a higher degree of heterogeneity in the headgroup region of the SM bilayers than in DPPC bilayers (cf. (Bagatolli et al., 1997)), but it could also derive from excited state reaction (Lakowicz, 1999). At present we cannot determine which explanation is more plausible. The matter is further complicated by the fact that SM and DHSM are both hydrogen donors and acceptors, whereas DPPC and Laurdan are hydrogen acceptors. Thus, hydrogen bonds between Laurdan and SM or DHSM are possible, but not between DPPC and Laurdan. Compared to previously published emission spectra of Laurdan in SM membranes (Bagatolli et al., 1999; Massey, 2001), the spectra we present are broader and more red shifted. However, the cited studies were performed at lower temperatures (23 and 25°C, respectively) compared to the present study. We also recorded emission spectra at 23°C that were more blue shifted and not as broad as at 36°C (results not shown). In the liquid-crystalline phase, the emission spectra of Laurdan were similar in the SM bilayers, whereas it was a little broader in the blue end in DPPC bilayers. This trend has also been shown in other studies (Bagatolli et al., 1999; Massey, 2001).

Membrane partitioning of Prodan

Prodan differs from Laurdan by having a shorter acyl chain (three carbon atoms) compared to Laurdan (12 carbon atoms). Based on this difference, Laurdan and Prodan detect membrane properties at different depths, e.g., the phospholipid polar headgroup pretransition is observable only with Prodan (Krasnowska et al., 1998). In the gel phase, Prodan had a blue-shifted emission spectra in the SM compared to DPPC vesicles, indicating that the probe had a less polar surrounding in SM membranes than in DPPC membranes. Massey showed similar spectra in a report where the Prodan emission in bovine brain SM and DPPC bilayers was compared (Massey, 2001). The emission spectra of Prodan from a DPPC membrane in the liquid-crystalline phase were, as in the gel phase, red shifted in relation to those recorded from comparable SM membranes.

The emission spectra of Prodan are very dependent on the degree of probe partitioning between solvent and the host membrane. It was observed, based on both steady-state and time-resolved measurements, that Prodan partitioned differently between water and the different membranes studied. Prodan partitioning into the highly ordered 16:0-DHSM membranes was less extensive than into e.g., 16:0-SM. This finding is actually expected, because we have shown that

detergent partitioning into DHSMs is significantly hindered as compared to the less-ordered SMs (Ollila and Slotte, 2002).

An interesting observation on the fluorescence properties of Prodan was that the fluorescence lifetimes were shorter in SM and DHSM bilayers than in DPPC membranes, although the emission spectra in SM and DHSM membranes were blue shifted compared to the DPPC membranes. Normally a blue shift of the emission spectrum is expected to result in longer lifetimes. It is unclear what caused the unusual behavior of Prodan in SM and DHSM membranes, but we see it as an indication of interfacial differences between PC and SM membranes, similar to those discussed earlier concerning Laurdan emission spectra.

In conclusion, this study with acyl-chain defined phospholipids has clearly shown that DHSMs are more ordered than their counterparts containing the *trans* 4 double bond in the sphingoid long-chain base. DHSM membranes also resist partitioning of amphiphilic molecules to a greater extent than the SM counterparts (this study and Ollila and Slotte, 2002). The interpretation of the interfacial data was not, however, straightforward. The complications were due to the partially unknown position of the probes in the different membranes, and the possible hydrogen bonds between probes and the SMs. However, the interfacial properties of SM or DHSM membranes differed clearly from the interfacial properties of DPPC membranes, most likely due differences in the hydrogen-bonding properties of the SMs and the glycerophospholipids. The differences between properties of DHSM and SM membranes were not as clear, especially in the liquid-crystalline phase. However, both Laurdan and Prodan reported small differences in the gel phase.

Because of the ordering properties of DHSM in membranes, further studies are warranted to examine the functional role of this particular sphingomyelin species, especially with respect to its possible participation in the formation of raft structures in cell membranes.

REFERENCES

Abbott, A. J., and G. L. Nelsestuen. 1987. Association of a protein with membrane vesicles at the collisional limit: studies with blood coagulation factor va light chain also suggest major differences between small and large unilamellar vesicles. *Biochemistry*. 26:7994–8003.

Andrich, M. P., and J. M. Vanderkooi. 1976. Temperature dependence of 1,6-diphenyl-1,3,5-hexatriene fluorescence in phophoslipid artificial membranes. *Biochemistry*. 15:1257–1261.

Asuncion-Punzalan, E., K. Kachel, and E. London. 1998. Groups with polar characteristics can locate at both shallow and deep locations in membranes: the behavior of dansyl and related probes. *Biochemistry*. 37:4603–4611.

Bagatolli, L. A., E. Gratton, and G. D. Fidelio. 1998. Water dynamics in glycosphingolipid aggregates studied by LAURDAN fluorescence. *Biophys. J.* 75:331–341.

Bagatolli, L. A., B. Maggio, F. Aguilar, C. P. Sotomayor, and G. D. Fidelio. 1997. Laurdan properties in glycosphingolipid-phospholipid mixtures: a comparative fluorescence and calorimetric study. *Biochim. Biophys. Acta*. 1325:80–90.

Bagatolli, L. A., T. Parasassi, G. D. Fidelio, and E. Gratton. 1999. A model for the interaction of 6-lauroyl-2-(N,N-dimethylamino)naphthalene with lipid environments: implications for spectral properties. *Photochem. Photobiol*. 70:557–564.

Barenholz, Y. 1984. Sphingomyelin-lecithin balance in membranes: composition, structure, and function relationships. *Physics of Membrane Fluidity*. 1:131–173.

Barenholz, Y., J. Suurkuusk, D. B. Mountcastle, T. E. Thompson, and R. L. Biltonen. 1976. A calorimetric study of the thermotropic behavior of aqueous dispersions of natural and synthetic sphingomyelins. *Biochemistry*. 15:2441–2447.

Barrow, D. A., and B. R. Lentz. 1985. Membrane structural domains. Resolution limits using diphenylhexatrien fluorescence decay. *Biophys. J*. 48:221–234.

Bernsdorff, C., A. Wolf, R. Winter, and E. Gratton. 1997. Effect of hydrostatic pressure on water penetration and rotational dynamics in phospholipid-cholesterol bilayers. *Biophys. J*. 72:1264–1277.

Bittman, R., C. R. Kasireddy, P. Mattjus, and J. P. Slotte. 1994. Interaction of cholesterol with sphingomyelin in monolayers and vesicles. *Biochemistry*. 33:11776–11781.

Brown, D. A., and J. K. Rose. 1992. Sorting of GPI-anchored proteins to glycolipid-enriched membrane subdomains during transport to the apical cell surface. *Cell*. 68:533–544.

Brown, R. E. 1998. Sphingolipid organization in biomembranes: what physical studies of model membranes reveal. *J. Cell Sci*. 111:1–9.

Byrdwell, W. C., and D. Borchman. 1997. Liquid chromatography/mass-spectrometric characterization of sphingomyelin and dihydro-sphingomyelin of human lens membranes. *Ophthalmic Res*. 29:191–206.

Cohen, R., Y. Barenholz, S. Gatt, and A. Dagan. 1984. Preparation and characterization of well defined D-erythro sphingomyelins. *Chem. Phys. Lipids*. 35:371–384.

Epand, R. M., and B. T. Leon. 1992. Hexagonal phase forming propensity detected in phospholipid bilayers with fluorescent probes. *Biochemistry*. 31:1550–1554.

Ferguson-Yankey, S. R., D. Borchman, K. G. Taylor, D. B. DuPre, and M. C. Yappert. 2000. Conformational studies of sphingolipids by NMR spectroscopy. I. Dihydrosphingomyelin. *Biochim. Biophys. Acta*. 1467:307–325.

Fiorini, R., M. Valentino, S. Wang, M. Glaser, and E. Gratton. 1987. Fluorescence lifetime distributions of 1,6-diphenyl-1,3,5-hexatriene in phospholipid vesicles. *Biochemistry*. 26:3864–3870.

Ho, C., S. J. Slater, and C. D. Stubbs. 1995. Hydration and order in lipid bilayers. *Biochemistry*. 34:6188–6195.

Ho, C., and C. D. Stubbs. 1997. Effect of n-alkanols on lipid bilayer hydration. *Biochemistry*. 36:10630–10637.

Jendrasiak, G. L., and R. L. Smith. 2001. The effect of the choline head group on phospholipid hydration. *Chem. Phys. Lipids*. 113:55–66.

Kaiser, R. D., and E. London. 1998. Location of diphenylhexatriene (DPH) and its derivatives within membranes: comparison of different fluorescence quenching analyses of membrane depth. *Biochemistry*. 37:8180–8190.

Kalb, E., F. Paltauf, and A. Hermetter. 1989. Fluorescence lifetime distributions of diphenylhexatriene-labeled phosphatidylcholine as a tool for the study of phospholipid-cholesterol interactions. *Biophys. J*. 56:1245–1253.

Kaluzny, M. A., L. A. Duncan, M. V. Merritt, and D. E. Epps. 1985. Rapid separation of lipid classes in high yield and purity using bonded phase columns. *J. Lipid Res*. 26:135–140.

Kinnunen, P. K. J. 1991. On the principles of functional ordering in biological membranes. *Chem. Phys. Lipids*. 57:375–399.

Krasnowska, E. K., L. A. Bagatolli, E. Gratton, and T. Parasassi. 2001. Surface properties of cholesterol-containing membranes detected by Prodan fluorescence. *Biochim. Biophys. Acta*. 1511:330–340.

Krasnowska, E. K., E. Gratton, and T. Parasassi. 1998. Prodan as a membrane surface fluorescence probe: partitioning between water and phospholipid phases. *Biophys. J*. 74:1984–1993.

Kuikka, M., B. Ramstedt, H. Ohvo-Rekila, J. Tuuf, and J. P. Slotte. 2001. Membrane properties of D-erythro-N-acyl sphingomyelins and their corresponding dihydro species. *Biophys. J*. 80:2327–2337.

Lakowicz, J. R. 1999. Principles of Fluorescence Spectroscopy. Kluvert Academic/Plenum Publishers, New York.

Lentz, B. R. 1989. Membrane ''fluidity'' as detected bydiphenylhexatriene probes. *Chem. Phys. Lipids*. 50:171–190.

Lentz, B. R., Y. Barenholz, and T. E. Thompson. 1976. Fluorescence depolarization studies of phase transitions and fluidity in phospholipid bilayers. 1. Single component phosphatidylcholine liposomes. *Biochemistry*. 15:4521–4528.

London, E., and D. A. Brown. 2000. Insolubility of lipids in Triton X-100: physical origin and relationship to sphingolipid/cholesterol membrane domains (rafts). *Biochim. Biophys. Acta*. 1508:182–195.

Massey, J. B. 2001. Interaction of ceramides with phosphatidylcholine, sphingomyelin and sphingomyelin/cholesterol bilayers. *Biochim. Biophys. Acta*. 1510:167–184.

Massey, J. B., and H. J. Pownall. 1998. Surface properties of native human plasma lipoproteins and lipoprotein models. *Biophys. J*. 74:869–878.

McMullen, T. P. W., R. N. A. H. Lewis, and R. N. McElhaney. 1993. Differential scanning calorimetric study of the effect of cholesterol on the thermotropic phase behavior of a homologous series of linear saturated phosphatidylcholines. *Biochemistry*. 32:516–522.

Nyholm, T., and J. P. Slotte. 2001. Comparison of Triton X-100 penetration into phosphatidylcholine and sphingomyelin mono- and bilayers. *Langmuir*. 17:4724–4730.

Ohvo-Rekila, H., B. Ramstedt, P. Leppimaki, and J. P. Slotte. 2002. Cholesterol interactions with phospholipids in membranes. *Prog. Lipid Res*. 41:66–97.

Ollila, F., and J. P. Slotte. 2002. Partitioning of Triton X-100, deoxycholate and C(10)EO(8) into bilayers composed of native and hydrogenated egg yolk sphingomyelin. *Biochim. Biophys. Acta*. 1564:281–288.

Pap, E. H., J. J. ter Horst, A. van Hoek, and A. J. Visser. 1994. Fluorescence dynamics of diphenyl-1,3,5-hexatriene-labeled phospholipids in bilayer membranes. *Biophys. Chem*. 48:337–351.

Parasassi, T., M. Di Stefano, M. Loiero, G. Ravagnan, and E. Gratton. 1994. Cholesterol modifies water concentration and dynamics in phospholipid bilayers: a fluorescence study using Laurdan probe. *Biophys. J*. 66:763–768.

Parasassi, T., E. Gratton, W. M. Yu, P. Wilson, and M. Levi. 1997. Two-photon fluorescence microscopy of laurdan generalized polarization domains in model and natural membranes. *Biophys. J*. 72:2413–2429.

Parente, R. A., and B. R. Lentz. 1985. Advantages and limitations of 1-palmitoyl-2-[[2-[4- (6-phenyl-trans- 1,3,5-hexatrienyl)phenyl]ethyl]-carbonyl]-3- sn-phosphatidylcholine as a fluorescent membrane probe. *Biochemistry*. 24:6178–6185.

Ramstedt, B., P. Leppimaki, M. Axberg, and J. P. Slotte. 1999. Analysis of natural and synthetic sphingomyelins using high-performance thin-layer chromatography. *Eur. J. Biochem*. 266:997–1002.

Ramstedt, B., and J. P. Slotte. 1999. Interaction of cholesterol with sphingomyelins and acyl-chain-matched phosphatidylcholines: a comparative study of the effect of the chain length. *Biophys. J*. 76:908–915.

Rottenberg, H. 1992. Probing the interactions of alcohols with biological membranes with the fluorescent probe Prodan. *Biochemistry*. 31:9473–9481.

Saito, H., I. Arimoto, M. Tanaka, T. Sasaki, T. Tanimoto, S. Okada, and T. Handa. 2000. Inhibition of lipoprotein lipase activity by sphingomyelin: role of membrane surface structure. *Biochim. Biophys. Acta*. 1486:312–320.

Sankaram, M. B., and T. E. Thompson. 1990. Interaction of cholesterol with various glycerophospholipids and sphingomyelin. *Biochemistry.* 29:10670–10675.

Sarmientos, F., G. Schwarzmann, and K. Sandhoff. 1985. Direct evidence by carbon-13 NMR spectroscopy for the erythro configuration of the sphingoid moiety in Gaucher cerebroside and other natural sphingolipids. *Eur. J. Biochem.* 146:59–64.

Schneider, P. B., and E. P. Kennedy. 1967. Sphingomyelinase in normal human spleens and in spleens from subjects with Niemann-Pick disease. *J. Lipid Res.* 8:202–209.

Schroeder, R., E. London, and D. Brown. 1994. Interactions between saturated acyl chains confer detergent resistance on lipids and glycosylphosphatidylinositol (GPI)-anchored proteins: GPI- anchored proteins in liposomes and cells show similar behavior. *Proc. Natl. Acad. Sci. USA.* 91:12130–12134.

Shinitzky, M., and Y. Barenholz. 1978. Fluidity parameters of lipid regions determined by fluorescence polarization. *Biochim. Biophys. Acta.* 515:367–394.

Simons, K., and E. Ikonen. 1997. Functional rafts in cell membranes. *Nature.* 387:569–572.

Slotte, J. P. 1999. Sphingomyelin-cholesterol interactions in biological and model membranes. *Chem. Phys. Lipids.* 102:13–27.

Small, D. M. 1986. The Physical Chemistry of Lipids, Handbook of Lipid Research. Plenum Press, New York.

Stryer, L. 1966. Excited-state proton-transfer reactions. A deuterium iso-tope effect on fluorescence. *J. Am. Chem. Soc.* 88:5708–5712.

Talbott, C. M., I. Vorobyov, D. Borchman, K. G. Taylor, D. B. DuPre, and M. C. Yappert. 2000. Conformational studies of sphingolipids by NMR spectroscopy. II. Sphingomyelin. *Biochim. Biophys. Acta.* 1467:326–337.

Veiga, M. P., J. L. Arrondo, F. M. Goni, A. Alonso, and D. Marsh. 2001. Interaction of cholesterol with sphingomyelin in mixed membranes containing phosphatidylcholine, studied by spin-label ESR and IR spectroscopies. A possible stabilization of gel-phase sphingolipid domains by cholesterol. *Biochemistry.* 40:2614–2622.

Weber, G., and F. J. Farris. 1979. Synthesis and spectral properties of a hydrophobic fluorescent probe: 6-propionyl-2-(dimethylamino)naph-thalene. *Biochemistry.* 18:3075–3078.

Williams, B. W., and C. D. Stubbs. 1988. Properties influencing fluorophore lifetime distributions in lipid bilayers. *Biochemistry.* 27:7994–7999.

Zeng, J. W., and P. L. Chong. 1991. Interactions between pressure and ethanol on the formation of interdigitated DPPC liposomes: a study with Prodan fluorescence. *Biochemistry.* 30:9485–9491.